Surface & Coatings Technology 226 (2013) 100–107

Contents lists available at SciVerse ScienceDirect

Surface & Coatings Technology

journal homepage: www.elsevier.com/locate/surfcoat

Effect of duty cycle and applied current frequency on plasma electrolytic oxidation (PEO) coating growth behavior

Vahid Dehnavi [a,*], Ben Li Luan [b,c,1], David W. Shoesmith [c,d,2], Xing Yang Liu [b,3], Sohrab Rohani [a,4]

[a] Department of Chemical and Biochemical Engineering, University of Western Ontario, London, ON, N6A 5B9, Canada
[b] National Research Council Canada, 800 Collip Circle, London, ON, N6G 4X8, Canada
[c] Department of Chemistry, University of Western Ontario, London, ON, N6A 5B7, Canada
[d] Surface Science Western, University of Western Ontario, 999 Collip Circle, London, ON, N6G 0J3, Canada

ARTICLE INFO

Article history:
Received 14 January 2013
Accepted in revised form 26 March 2013
Available online 4 April 2013

Keywords:
Plasma electrolytic oxidation
Aluminum
Duty cycle
Frequency

ABSTRACT

Ceramic coatings were created on the surface of 6061 aluminum alloy using a plasma electrolytic oxidation (PEO) process employing a pulsed direct current (DC) power mode in an alkaline electrolyte. The effect of electrical parameters including frequency and duty cycle on the microdischarge behavior and coating growth was investigated at constant current. Surface features of coatings were studied using scanning electron microscopy. Energy dispersive spectroscopy was employed to investigate elemental distribution on the coating surfaces and cross-sections. Applying lower duty cycles was found to result in increased breakdown voltages and microdischarges with higher spatial density and lower intensity. Further, applying a lower duty cycle was also found to promote the uniformity of silicon distribution in the coating. Based on these new findings, a new conceptual model is proposed to explain the concentration distribution of Si on the surface of coatings prepared at different duty cycles.

1. Introduction

Light metals, especially aluminum and magnesium alloys, are finding increasing applications in different industries such as automotive and aerospace because of their strength to weight ratio, low density compared to steel, ease of fabrication and recycling potential. In the automotive industry, for instance, a total of about 110 kg of aluminum used per vehicle in 1996 is predicted to rise to 250–340 kg by 2015. These metals require careful finishing to produce surface coatings with adequate resistance to both wear and corrosion because they are reactive and have low hardness [1,2].

A relatively novel technique to create functional oxide layers on light metals, which has generated growing interest recently, is plasma electrolytic oxidation (PEO), also called micro-arc oxidation (MAO) [3], anodic oxidation by spark discharge [4] or spark anodizing [5–8]. The PEO process uses the same configuration as conventional anodizing but is operated at much higher potentials, usually in the range 400–700 V, and involves many short-lived microdischarges as a result of localized dielectric breakdown of the growing coating [8,9]. PEO provides coatings with better characteristics compared to conventional and hard anodizing procedures. The coatings produced by conventional anodizing are not thick enough to provide effective protection against wear and corrosion and therefore are used mainly for decoration. The PEO method is capable of producing thicker coatings with higher hardness, better wear and corrosion resistance and great bonding strength with the substrate as compared to the conventional anodizing method. The electrolyte used in PEO is typically a low concentration alkaline solution which is more environmentally friendly than a hard anodizing process employing strong acids [10,11].

Since the discharge events are very short in PEO, it is very difficult to catch instantaneously the discharge event to analyze the physical and chemical processes occurring in the discharge channels. As a result, controversy exists over the growth mechanism of PEO coatings [10]. In an earlier work [12], three models were suggested to explain discharge formation: (1) microdischarges are the result of oxide film dielectric breakdown in a strong electric field; (2) microdischarges occur due to gas discharges in micro pores in the oxide film; (3) free electron generation and contact glow discharge. In a recent work [13], using optical emission spectroscopy (OES), a discharge model based on the locations of discharge initiation was proposed. This model assumes three types of discharge, types A, B and C. Type B discharges originate from the metal-oxide interface and are strong as a result of dielectric breakdown through the oxide layer creating cratered structures. Types A and C, originating from the oxide-electrolyte interface, are weaker than type B discharges, and occur as a result of gas discharges in micro pores in the oxide layer.

* Corresponding author. Tel.: +1 519 702 5586.
E-mail addresses: vdehnavi@uwo.ca, vdehnavi@gmail.com (V. Dehnavi), Ben.Luan@nrc-cnrc.gc.ca (B.L. Luan), dwshoesm@uwo.ca (D.W. Shoesmith), XingYang.Liu@nrc-cnrc.gc.ca (X.Y. Liu), srohani@uwo.ca (S. Rohani).
[1] Tel.: +1 519 430 7043.
[2] Tel.: +1 519 661 2111x86366.
[3] Tel.: +1 519 430 7042.
[4] Tel.: +1 519 661 4116.

0257-8972/$ – see front matter © 2013 Published by Elsevier B.V.
http://dx.doi.org/10.1016/j.surfcoat.2013.03.041

Discharges play a very important role in the coating growth mechanism. Several investigations have been conducted to characterize discharge behavior during PEO using different methods. Digital imaging [9,12,14] revealed that, as the PEO process proceeds microdischarge intensity increases while their spatial density decreases. Yerokhin et al. [12] estimated the mean value of current density passing through a discharge to be between 18 and 50 kA/m^2. Mécuson et al. [15] used a pulse bipolar current mode with different ratios of positive to negative charge density. Using a video camera, they observed that when a higher negative than positive charge was applied, the intensity of microdischarges decreased in the later stages of the PEO process and a "softer" sparking resulted.

Hussein et al. [7,13] applied optical emission spectroscopy using different current modes. They found that electrical parameters (current density, frequency and duty cycle) and process time affect the plasma temperature as a result of different types of discharges such as dielectric breakdown and gas discharges. They estimated the average temperature of discharges to be in the 4900–5400 K range while strong discharges can produce temperatures in the range 6000–10000 K.

To justify industrial application of PEO, a more systematic and in-depth study of the influence of various parameters on the process is required. Many previous studies have investigated the effects of electrolyte composition [16–19] and current mode [20–22] on the produced coatings. However, information on the role of electrical parameters such as frequency and duty cycle is limited in the literature. The present study investigates the effect of frequency and duty cycle on the coating growth behavior during PEO.

2. Experimental procedure

Disk samples with a diameter of about 3 cm and a thickness of 7–9 mm were cut from a 6061-T651 aluminum alloy bar supplied by Kaiser Aluminum, USA. To ensure a reproducible initial surface condition, samples were polished with 600 grit emery polishing paper followed by degreasing in propanol and rinsing with distilled water. A PEO unit custom-built by the National Research Council Canada (NRC, Vancouver, Canada) equipped with a DC power supply was used to produce the coatings. The positive output of the power supply was connected to the sample immersed in the electrolyte serving as the working electrode (anode) and the negative output was connected to the stainless steel electrolyte container acting as the counter electrode (cathode). To ensure a good connection between the power supply and the samples, a threaded hole was drilled on one side of each sample. Then the sample was bolted to a steel rod (insulated by a ceramic jacket from the electrolyte) connected to the power supply. PEO coatings were produced using the uni-polar pulsed DC mode with a square waveform applied at different power frequencies of 50, 500, 1000 and 2000 Hz. Two duty cycles (D_t), 80% and 20%, were used. At the frequency of 1000 Hz two additional duty cycles of 10% and 50% were also used. The duty cycle is defined as:

$$D_t = [t_{on}/(t_{on} + t_{off})] \times 100$$

where t_{on} is the 'on' duration and t_{off} is the 'off' duration during a single cycle.

The PEO process was carried out at a constant current density of 1500 A/m^2 for 30 min for all samples. Table 1 lists the sample codes and the processing conditions.

The electrolyte was a solution of 2 g/L Na_2SiO_3 and 2 g/L KOH in deionized water with a pH of 12.5. The electrolyte temperature was maintained in the range of 33–38 °C during treatment using an external DCA 500 Durachill heat exchanger manufactured by Polyscience.

Coating thickness was evaluated using an Eddy current gauge. Twenty measurements were taken on the coated surface of each sample. Statistical treatments were applied to extract the mean data values and scatter.

Table 1
PEO process parameters and sample codes for coating deposition on 6061 Al alloy.

Sample code	Frequency (Hz)	Duty cycle (%)	t_{on} (ms)	t_{off} (ms)
A2	50	20	4	16
A8	50	80	16	4
B2	500	20	0.4	1.6
B8	500	80	1.6	0.4
C1	1000	10	0.1	0.9
C2	1000	20	0.2	0.8
C5	1000	50	0.5	0.5
C8	1000	80	0.8	0.2
D2	2000	20	0.1	0.4
D8	2000	80	0.4	0.1

Coating surfaces and cross sections were examined using a LEO 440 scanning electron microscope (SEM) equipped with a Quartz EDX system and a Hitachi S-3500N SEM equipped with an Oxford Instruments 7490 X-ray detector. The samples were sputter-coated with gold prior to SEM imaging to minimize surface charging.

3. Results and discussion

3.1. Voltage–time response

Voltage–time responses for PEO coatings formed using the various duty cycles and frequencies are shown in Fig. 1. As previously reported [16,19,23,24], an initial linear, abrupt voltage increase occurs within a short period of time (about 15 s) followed by a sudden reduction in slope of the voltage–time curve. The point at which the slope of the voltage–time curve changes is designated the sparking or breakdown voltage.

The PEO process is accompanied by sparking microdischarges as a result of dielectric breakdown [13,25], gas discharge [13], contact glow discharge [12] or any of their combinations which is a unique feature of PEO as compared to conventional anodization [25].

Throughout the PEO process the color, intensity and density of micro discharges constantly change. The color of the microdischarges changes from bluish white to yellow and eventually to orange while the intensity increases and the density decreases [3,11,26].

The sparking or breakdown voltage as well as the maximum voltage eventually achieved (Fig. 1) were higher in samples treated at a duty cycle of 20% compared to those treated at a duty cycle of 80%. Fig. 2 demonstrates the effect of duty cycle on the voltage–time response of coatings grown at a frequency of 1000 Hz. Decreasing the duty cycle from 80% to 10% was found to result in higher breakdown and maximum voltages. At a duty cycle of 80%, the sparking and

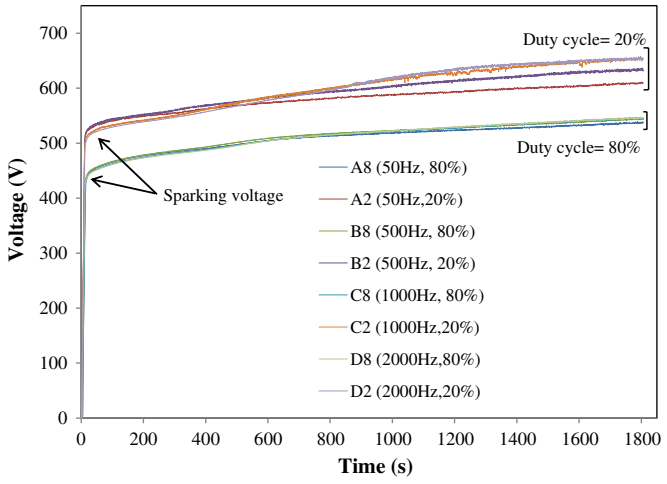

Fig. 1. Voltage–time response at duty cycles of 20% and 80%.

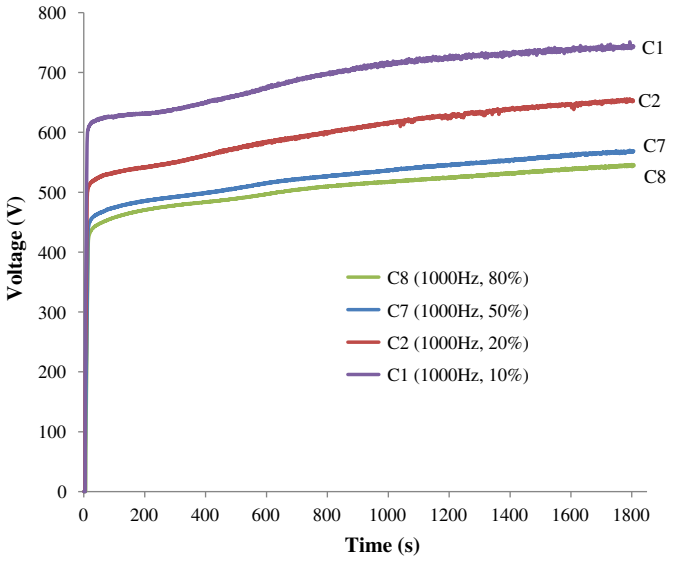

Fig. 2. Effect of duty cycle on voltage–time response at a frequency of 1000 Hz.

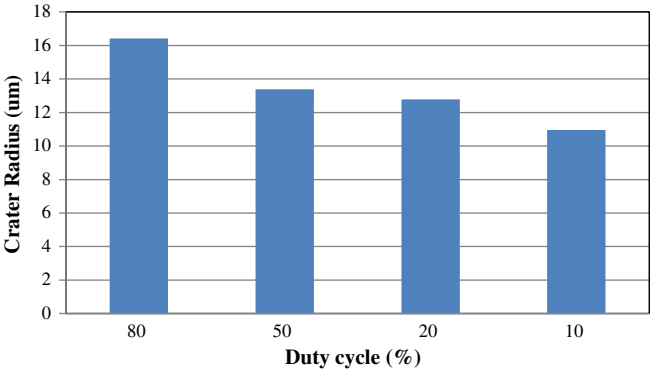

Fig. 4. Effect of duty cycle on the size of craters on the surface of PEO coated samples prepared at a frequency of 1000 Hz.

maximum voltages were 424 and 532 V respectively, while for a duty cycle of 10% the corresponding numbers rose to 594 and 759 V, respectively.

A comparison of the curves in Fig. 1 showed no considerable difference in sparking and maximum voltage reached during PEO of samples treated at the same duty cycle but different frequencies.

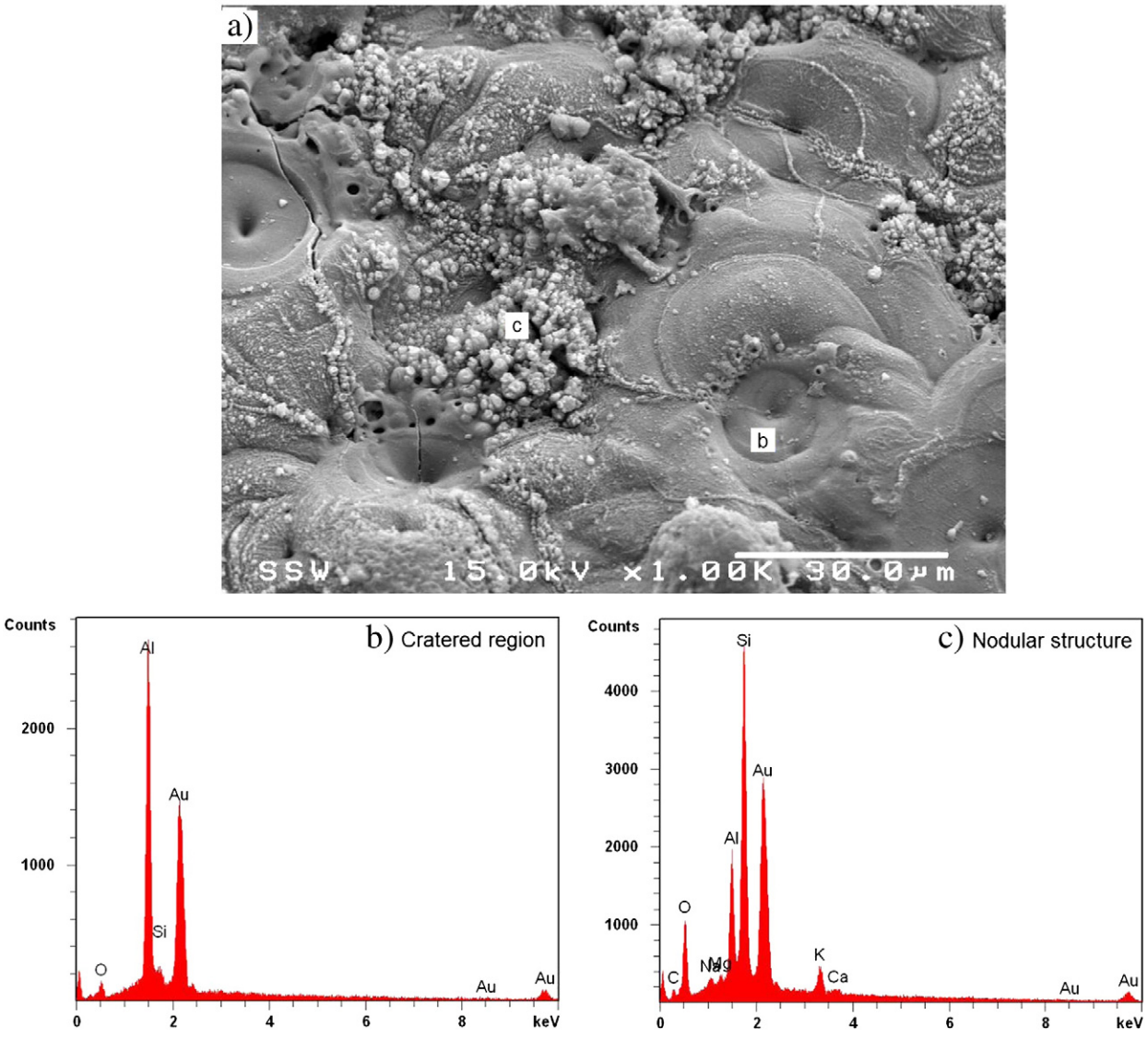

Fig. 3. (a) SEM images (secondary electron mode) of free surface of PEO coating on sample C8; (b) and (c) EDX analysis from regions "b" and "c" respectively.

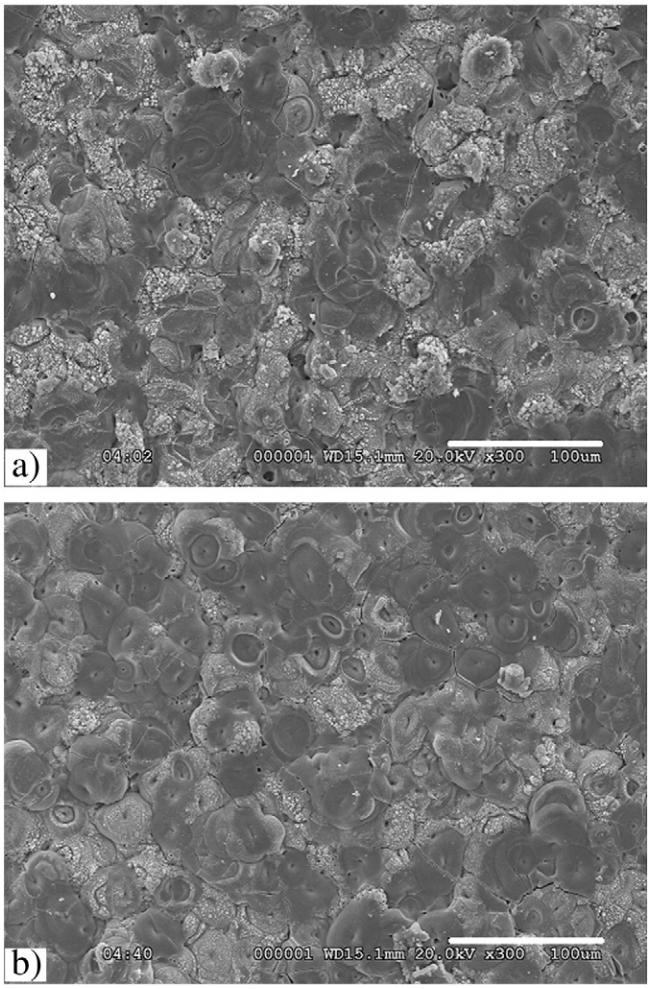

Fig. 5. SEM micrographs (BS mode) of PEO coating surfaces, (a) C8, 80% duty cycle; and (b) C2, 20% duty cycle.

3.2. Coating surface morphology and composition

A typical SEM micrograph of a coated surface is illustrated in Fig. 3-a. Two distinct regions can be observed on the surface of all samples: a cratered structure with a central hole (Area "b") and a lighter area with a nodular structure (Area "c"). The central hole in the cratered region is a discharge channel through which molten material was ejected from the coating/substrate interface due to the high temperature and strong electric field. After ejection this material rapidly solidified upon contact with the electrolyte.

EDX spectra measured at these two characteristic regions are presented in Fig. 3-b and c. The cratered region is rich in aluminum, consistent with its ejection through the film from the substrate/coating interface. The nodular structure is rich in Si suggesting that it is formed by the codeposition of aluminum and silicon in the solution.

It is generally believed [3,15,27] that the coating growth is the result of the flow of oxidized molten aluminum through discharge channels. The discharges created during PEO play a key role in the coating growth [8]. The size and surface features of the craters could be a reflection of the density and intensity of the discharges [7,13]; i.e., the stronger the discharges, the bigger the craters. Fig. 4 illustrates the effect of the duty cycle on the size of craters (the average standard deviation of measured crater sizes was 2.8 μm). Image analysis software (MIP from Metsofts) was employed to measure the size of craters in the SEM micrographs and the measured values were statistically treated and reported. Since the intensity of the microdischarges varies significantly during the PEO process, the values of the crater radii reported here show a general trend and should not be treated as quantitatively certain. It is observed (Fig. 4) that the crater size tends to increase with increasing duty cycle, which could indicate enhanced or intensified microdischarges as the duty cycle increases.

The effect of duty cycle on the surface morphologies of coatings formed at a frequency of 1000 Hz is presented in Fig. 5. Comparison of sample C8 (Fig. 5-a, 80% duty cycle) with sample C2 (Fig. 5-b, 20% duty cycle) shows that fewer craters are formed on C8 and the surface is more densely covered with nodular structures shown to be rich in Si by EDX analyses.

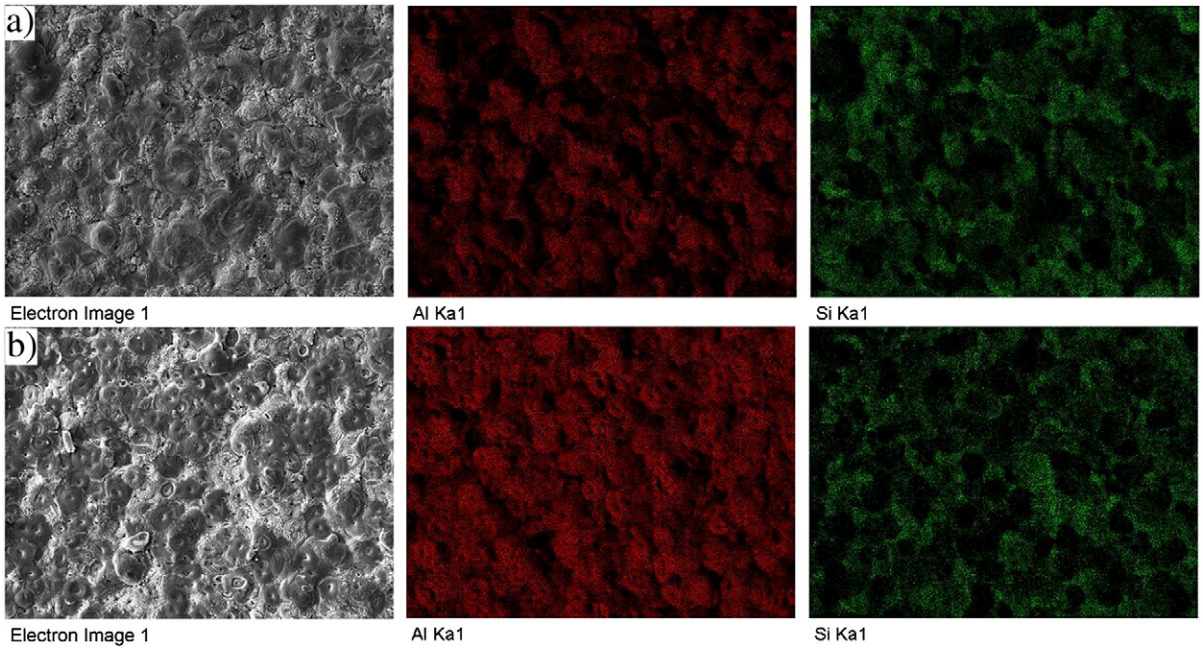

Fig. 6. Surface EDX elemental maps for (a) sample D8 (80% duty cycle); and (b) sample D2 (20% duty cycle).

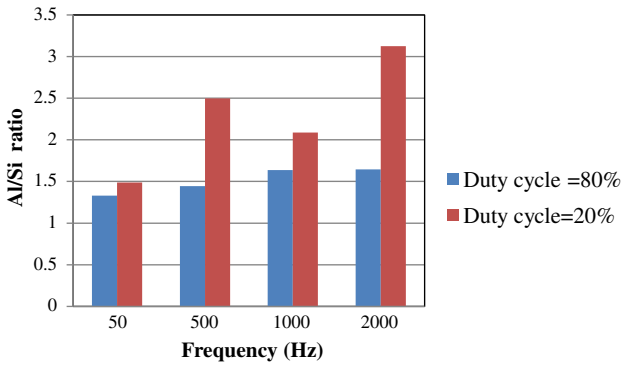

Fig. 7. Al/Si ratio calculated from surface EDX elemental maps.

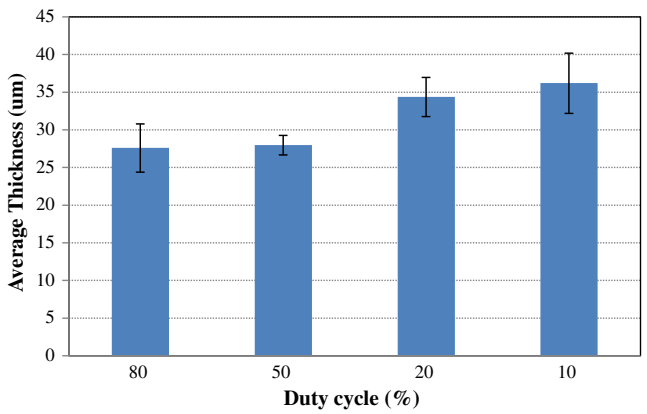

Fig. 9. Effect of duty cycle on coating thickness on samples coated at a frequency of 1000 Hz.

The EDX elemental surface maps of samples D2 (20% duty cycle) and D8 (80% duty cycle) are compared in Fig. 6. The accuracy of the elemental concentration measurements may vary between 2% and 7% [13]. It could be observed that a higher surface concentration of Al is obtained at a low, compared to a high, duty cycle (samples D2 and D8, respectively). On the contrary, the Si presence appears to be higher at a higher duty cycle, though this is not as obvious as in the case of Al. The Al/Si intensity ratios for different frequencies obtained from EDX elemental surface mapping (Fig. 7) reveal that this ratio increases with decreasing duty cycle, consistent with the observations from Fig. 6. This suggests that at a lower duty cycle more discharges occurred resulting in more Al participating in the discharging.

Visual observation of the sample surfaces at various stages of the coating process (Fig. 8) revealed that the population, size and color of microdischarge events vary throughout the oxidation process. At the beginning (Fig. 8-a and b) microdischarges are smaller with a bluish white color but grow in size and turn orange at later stages (Fig. 8-c and d). It was also observed that, at lower duty cycles (Fig. 8-b and d) microdischarges are less intense and have a higher spatial density at all stages of the process. The difference between the high and low duty cycles becomes more apparent at longer times (Fig. 8-c and d).

Yerokhin et al. [12] suggest the most likely cause of the microdischarge color change as the process continues could be due to ionic emission from the molten oxide film. As the coating thickens, less heat is transferred to the aluminum substrate since more is absorbed by the coating. The high heating rates developed in the anode make it possible for the oxide film to be partially melted, resulting in an ionic emission.

The results presented in Figs. 3 to 8 confirm that the intensity of the microdischarges decreases while their spatial density increases when a lower duty cycle is applied. As previously mentioned in Section 3.1, craters are the result of strong microdischarges caused by dielectric breakdowns of the coating that penetrate through its entire thickness. As such, the larger number of smaller craters at low duty cycles (Figs. 4 and 5) suggests a higher number of sparks with lower intensity. One possible explanation for the lower intensity of microdischarges at low duty cycles could be the higher number of sparks on the surface. As the number of microdischarges increases, the current passing through each individual microdischarge channel decreases because the overall current is kept constant, resulting in smaller crater sizes (Fig. 5).

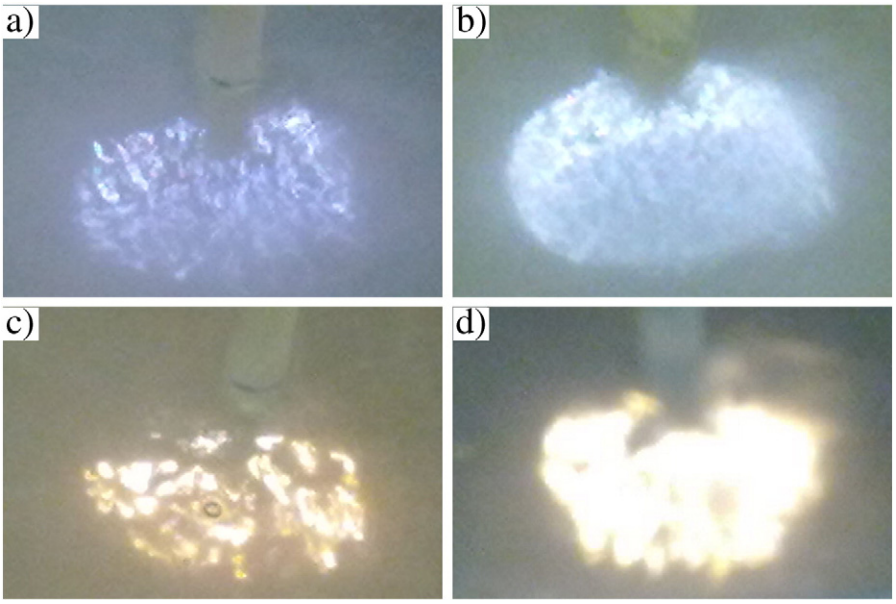

Fig. 8. Appearance of microdischarges during PEO; (a) C8 after 4 min , (b) C2 after 4 min , (c) C8 after 28 min, (d) C2 after 28 min.

3.3. Coating thickness

Thickness measurements (Fig. 9) show that the coating growth rate increases gradually with decreasing duty cycle at constant frequency. This increased growth rate at lower duty cycles could be linked to the fact that coating growth is the result of oxidized molten aluminum as it flows out through discharge channels and more discharges are involved at lower duty cycles. The cross sections of PEO coatings examined by SEM (Fig. 10-a and e) for samples treated at a frequency of 1000 Hz and duty cycles of 80% and 20% reveal some porosity and discharge channels within the coating. The porosity is assumed to be the result of dissolved oxygen being trapped in the

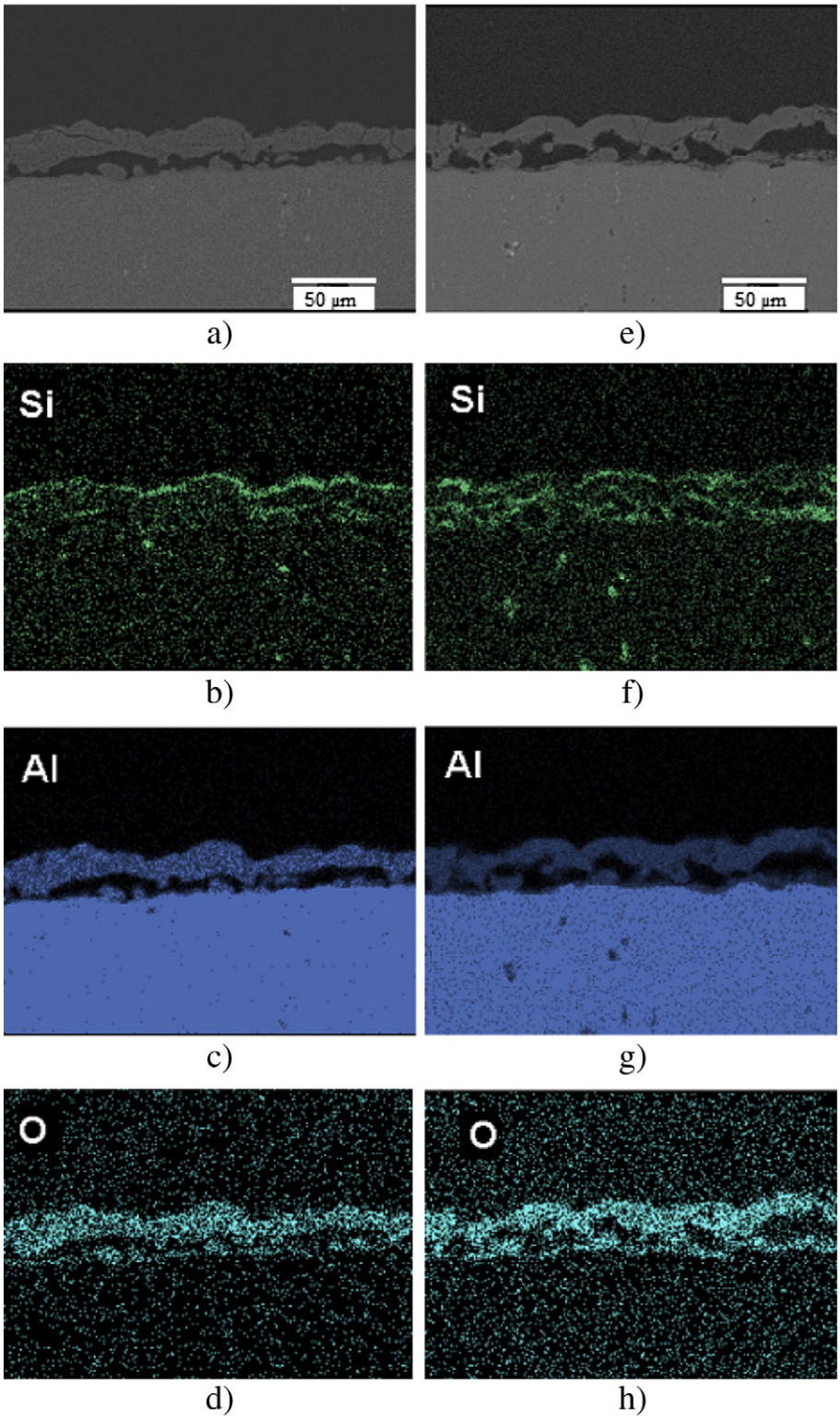

Fig. 10. Results of EDX on the cross sections of coatings. Sample C8 (a) Scanning electron micrograph (b) Silicon (c) Aluminum and (d) Oxygen elemental maps; Sample C2 (e) Scanning electron micrograph (f) Silicon (g) Aluminum and (h) Oxygen elemental maps.

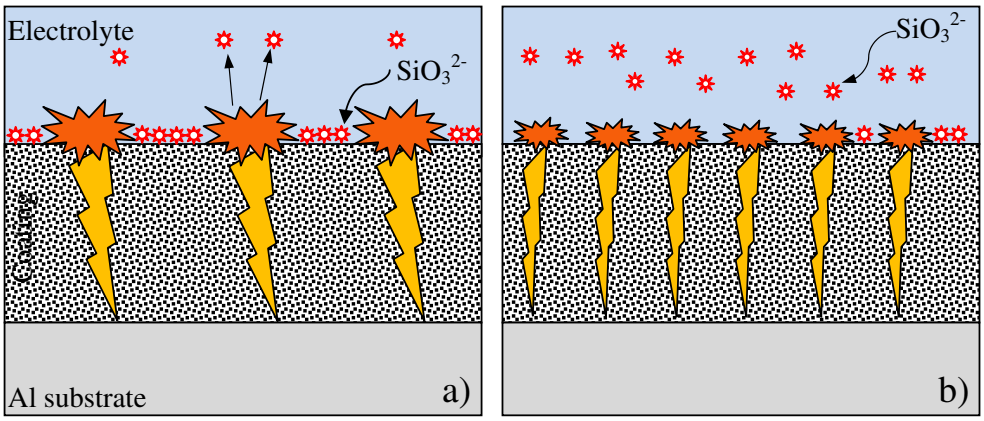

Fig. 11. Schematic diagrams showing the effect of microdischarge characteristics on the distribution of silicon on the surface of PEO coated samples for (a) high duty cycle and (b) low duty cycle conditions.

molten oxides [28]. It should be noted that the defects adjacent to the coating/substrate interface are the result of polishing during sample preparation and the coatings are not separated from the substrates.

3.4. Distribution of elements

SEM micrographs and EDX analyses of the coating cross sections for samples C8 and C2 are presented in Fig. 10. Comparison of the elemental maps does not detect any significant differences in the distribution of Al in the oxide coating but shows that the distribution of Si differs considerably in these two samples. When using a high duty cycle (C8), the Si is concentrated on the outer surface of the coating (Fig. 10-b), whereas at low duty cycles (C2, Fig. 10-f) Si is distributed more evenly within the coating.

The high concentration of Si at the coating surface in samples coated at high duty cycles could be linked to the microdischarge behavior during PEO. It was previously reported [5,14,24] that in electrolytes containing silicate, silicon species are concentrated closest to the coating surface. It has been proposed [10,16] that Si forms insoluble gels which reduce Si ionic mobility and as a result a silicon rich outer part is formed by deposition of this gel at the coating interface.

At low duty cycles the microdischarges are less intense and their spatial density is higher (Fig. 8-b and d) whereas at high duty cycles microdischarges are stronger with lower spatial density (Fig. 8-a and c). Each microdischarge ejects oxidized molten aluminum onto the surface. As a result of the force of these ejections, adsorbed negative ions on the surface, for instance SiO_3^{2-} or Si containing gels, as proposed by some researchers [10,16], would be detached from the surface. We propose a new schematic diagram in Fig. 11 showing how microdischarge spatial density could affect Si distribution on the surface. In Fig. 11-a, where sparks are further apart, Si containing species can be adsorbed on the surface of the anode (substrate) while in Fig. 11-b most of the Si containing species are detached from the surface due to the larger number of sparks on the surface.

The more uniform distribution of silicon across the ceramic coating could be ascribed to the higher electric fields produced in samples coated at lower duty cycles. Anions present in the electrolyte, SiO_3^{2-} for instance, enter the discharge channels under a strong electric field through electrophoresis [10]. Since a decrease in duty cycle results in higher electric fields (Figs. 1 and 2) and more sparks, the possibility of silicon entering discharge channels increases and results in a more uniform distribution.

4. Conclusion

The PEO processing of 6061 aluminum alloy using different frequencies and duty cycles was investigated. At low duty cycles the sparking and maximum voltages were both higher. Two regions were observed on the surface of all samples: a cratered region with discharge channels in the center and rich in aluminum implying craters were the result of dielectric breakdown across the coating; and a nodular structure, rich in silicon. Applying lower duty cycles produced microdischarges with higher spatial density and lower intensity. These softer microdischarges created smaller craters. During the PEO process when high duty cycles were applied, microdischarges became stronger but their number decreased, especially at longer times. However, at lower duty cycles the surface of the sample was totally covered by sparks even during the final stages. The sparking behavior caused by the application of different electrical parameters affected silicon distribution. Low duty cycles resulted in a lower concentration of Si on the surface and more uniform distribution of Si across the coating. This phenomenon could be ascribed to the higher density of sparks at low duty cycles which detaches adsorbed silicon containing species from the surface of the sample and also stronger electric fields which increase the possibility of incorporation of Si rich anions into the coating.

This report offers new observations about the growth behavior of PEO coatings. It is expected that the results presented here could be utilized to better control the PEO process in order to produce coatings with desired properties.

Acknowledgments

This research was supported by the National Research Council Canada (NRC) and the Natural Science and Engineering Research Council of Canada (NSERC) grants.

References

[1] F.C. Walsh, C.T.J. Low, R.J.K. Wood, K.T. Stevens, J. Archer, A.R. Poeton, A. Ryder, Trans. Inst. Met. Finish. 87 (3) (05-01-2009) 122.
[2] W.S. Miller, L. Zhuang, J. Bottema, A.J. Wittebrood, P. De Smet, A. Haszler, A. Vieregge, Mater. Sci. Eng., A 280 (1) (2000) 37.
[3] G. Sundararajan, L. Rama Krishna, Surf. Coat. Technol. 167 (2–3) (2003) 269.
[4] P. Kurze, W. Krysmann, H.G. Schneider, Cryst. Res. Technol. 21 (12) (1986) 1603.
[5] F. Monfort, A. Berkani, E. Matykina, P. Skeldon, G.E. Thompson, H. Habazaki, K. Shimizu, J. Electrochem. Soc. 152 (6) (2005) C382.
[6] V.S. Rudnev, M.A. Medkov, T.P. Yarovaya, N.I. Steblevskaya, P.M. Nedovzorov, M.V. Belobeletskaya, Russ. J. Appl. Chem. 85 (4) (2012) 621.
[7] R.O. Hussein, D.O. Northwood, X. Nie, J. Vac. Sci. Technol. A 28 (4) (2010) 766.
[8] C.S. Dunleavy, I.O. Golosnoy, J.A. Curran, T.W. Clyne, Surf. Coat. Technol. 203 (22) (2009) 3410.
[9] F. Mécuson, T. Czerwiec, T. Belmonte, L. Dujardin, A. Viola, G. Henrion, Surf. Coat. Technol. 200 (1–4) (2005) 804.
[10] B.L. Jiang, Y.M. Wang, in: H. Dong (Ed.), Surface engineering of light alloys: aluminum, Magnesium and titanium alloysCRC Press, 2010, p. 110.
[11] J.M. Wheeler, J.A. Curran, S. Shrestha, Surf. Coat. Technol. 207 (2012) 480.
[12] A.L. Yerokhin, L.O. Snizhko, N.L. Gurevina, A. Leyland, A. Pilkington, A. Matthews, J. Phys. D: Appl. Phys. 36 (17) (2003) 2110.

[13] R.O. Hussein, X. Nie, D.O. Northwood, A.L. Yerokhin, A. Matthews, J. Phys. D: Appl. Phys. 43 (2010) 105203.
[14] S. Moon, Y. Jeong, Corros. Sci. 51 (7) (2009) 1506.
[15] F. Mécuson, T. Czerwiec, G. Henrion, T. Belmonte, L. Dujardin, A. Viola, J. Beauvir, Surf. Coat. Technol. 201 (21) (2007) 8677.
[16] F. Monfort, A. Berkani, E. Matykina, P. Skeldon, G.E. Thompson, H. Habazaki, K. Shimizu, Corros. Sci. 49 (2) (2007) 672.
[17] Z. Wang, L. Wu, W. Cai, A. Shan, Z. Jiang, J. Alloys Compd. 505 (1) (2010) 188.
[18] A.A. Voevodin, A.L. Yerokhin, V.V. Lyubimov, M.S. Donley, J.S. Zabinski, Surf. Coat. Technol. 86-87 (Part 2) (1996) 516.
[19] G. Lv, W. Gu, H. Chen, W. Feng, M.L. Khosa, L. Li, E. Niu, G. Zhang, S. Yang, Appl. Surf. Sci. 253 (5) (2006) 2947.
[20] A.L. Yerokhin, A. Shatrov, V. Samsonov, P. Shashkov, A. Pilkington, A. Leyland, A. Matthews, Surf. Coat. Technol. 199 (2–3) (2005) 150.
[21] R.H.U. Khan, A. Yerokhin, X. Li, H. Dong, A. Matthews, Surf. Coat. Technol. 205 (6) (2010) 1679.
[22] Y. Guangliang, L. Xianyi, B. Yizhen, C. Haifeng, J. Zengsun, J. Alloys Compd. 345 (1–2) (2002) 196.
[23] K.M. Lee, Y.G. Ko, D.H. Shin, Curr. Appl. Phys. 11 (4, Supplement) (2011) S55.
[24] F. Monfort, E. Matykina, A. Berkani, P. Skeldon, G.E. Thompson, H. Habazaki, K. Shimizu, Surf. Coat. Technol. 201 (21) (2007) 8671.
[25] H. Wu, J. Wang, B. Long, B. Long, Z. Jin, W. Naidan, F. Yu, D. Bi, Appl. Surf. Sci. 252 (5) (2005) 1545.
[26] A.L. Yerokhin, X. Nie, A. Leyland, A. Matthews, S.J. Dowey, Surf. Coat. Technol. 122 (2–3) (1999) 73.
[27] L. Rama Krishna, K.R.C. Somaraju, G. Sundararajan, Surf. Coat. Technol. 163–164 (2003) 484.
[28] J.A. Curran, T.W. Clyne, Acta Mater. 54 (7) (2006) 1985.